

Enhanced tunneling magnetoresistance of Fe₃O₄ in a Fe₃O₄-hexabromobenzene (C₆Br₆) composite system

Wendong Wang, Jibao He, and Jinke Tang

Citation: *Journal of Applied Physics* **105**, 07B105 (2009); doi: 10.1063/1.3072779

View online: <http://dx.doi.org/10.1063/1.3072779>

View Table of Contents: <http://scitation.aip.org/content/aip/journal/jap/105/7?ver=pdfcov>

Published by the [AIP Publishing](#)

Articles you may be interested in

Temperature driven transition from giant to tunneling magneto-resistance in Fe₃O₄/Alq₃/Co spin Valve: Role of Verwey transition of Fe₃O₄

J. Appl. Phys. **115**, 17C110 (2014); 10.1063/1.4862845

Comment on “Inversed tunneling magnetoresistance in hybrid FePt/Fe₃O₄ core/shell nanoparticles systems” [*J. Appl. Phys.* **108**, 103905 (2010)]

J. Appl. Phys. **109**, 086101 (2011); 10.1063/1.3561507

Role of oxide barrier in intergranular tunnel junctions: An enhanced magnetoresistance in SiO₂ and ZnO coated Fe₃O₄ nanoparticle compacts

J. Appl. Phys. **103**, 07F318 (2008); 10.1063/1.2840902

Enhanced low field magnetoresistance of Fe₃O₄ nanosphere compact

J. Appl. Phys. **100**, 044314 (2006); 10.1063/1.2335386

Large room-temperature spin-dependent tunneling magnetoresistance in a Fe₃O₄-polymer composite system

J. Appl. Phys. **99**, 08J108 (2006); 10.1063/1.2165588



Enhanced tunneling magnetoresistance of Fe₃O₄ in a Fe₃O₄-hexabromobenzene (C₆Br₆) composite system

Wendong Wang,^{1,a)} Jibao He,² and Jinke Tang¹

¹Department of Physics & Astronomy, University of Wyoming, Laramie, Wyoming 82071, USA

²Coordinated Instrumentation Facility, Tulane University, New Orleans, Louisiana 70118, USA

(Presented 13 November 2008; received 21 September 2008; accepted 27 November 2008; published online 11 March 2009)

Magnetotransport of Fe₃O₄-hexabromobenzene (C₆Br₆) composite has been studied. Powders of C₆Br₆ and Fe₂O₃ nanoparticles were mixed together. They were annealed in hydrogen flow. There was a phase transformation from Fe₂O₃ to Fe₃O₄ after annealing. Giant negative magnetoresistance (MR) was observed at room temperature and the MR ratio is about 13.4% in an applied field of 5 T. The maximum MR ratio is 21.5% at 130 K. The temperature dependence of the resistivity exhibits characteristics of intergranular tunneling in the samples. The enhancement of the MR ratio is attributed to the fact that the C₆Br₆ can act as barrier material and, more importantly, can prevent the oxidation of the surface of Fe₃O₄, which is believed to alter the half-metallic state at the surface. © 2009 American Institute of Physics. [DOI: 10.1063/1.3072779]

I. INTRODUCTION

There has been increased interest in the half-metallic magnetite (Fe₃O₄) due to its highly spin polarized nature (supposedly ~100%).^{1,2} In principle, a high spin polarization should result in large tunneling magnetoresistance (TMR) since the latter is proportional to the spin polarization of the tunneling electrons.³⁻⁵ Many studies have focused on the magnetoresistance (MR) ratio in Fe₃O₄ of different forms including epitaxial and polycrystalline films, powders, and tunnel junctions.⁶⁻¹⁰ In early reports, some groups have claimed a large MR response on breaking contact of two microscaled single crystals of magnetite¹¹ and thin film structure composed of a few stacked monolayers of organically encapsulated magnetite nanocrystals.¹² However, in most cases the MR ratio is much smaller than expected, especially at room temperature. In fact, it is well known that in polycrystalline specimens and powder compacts of Fe₃O₄, the surfaces or interfaces at the grain boundaries have rather different magnetic properties and reduced spin polarization compared to those of the bulk.¹³⁻¹⁶ This is a consequence of off-stoichiometry, surface reconstruction, oxidation, defects, and bonding effects located at or close to the surfaces and interfaces. Recently, some investigations have focused on improving MR performance of Fe₃O₄.¹⁷⁻²² Zeng *et al.*¹⁷ reported 35% MR at 60 K for ordered three-dimensional arrays of Fe₃O₄ nanoparticles with annealing in high vacuum. Rybchenko *et al.*¹⁹ showed enhancement in MR of bulk granular magnetite by annealing in paraffin wax. Lu *et al.*²⁰ found relatively large low field MR in ultrathin Fe₃O₄ nanocrystalline films by rapid thermal annealing at 800 °C for 120 s in pure nitrogen. These authors all used passive annealing process to prevent the surfaces or interfaces from oxidation.

We have previously reported that polystyrene (PS) coated magnetite nanoparticles exhibit drastically enhanced intergranular TMR.¹⁸ The large TMR results from the better

protection of the surfaces of Fe₃O₄ from oxidation by the PS coating. However the PS has low melting point (240 °C) and softening temperature (95 °C), which will limit its potential applications.

In this article, the investigation of the MR and spin polarization of the surface of Fe₃O₄ in a magnetite/organic hexabromobenzene (C₆Br₆) nanocomposite is discussed. The melting point of C₆Br₆ is relatively high (>320 °C) among oxygen-free organic materials. C₆Br₆ can also be deposited as molecular films,²³ so it has the potential to be applied to spin polarized thin film system for spintronic studies.

II. RESULTS AND DISCUSSION

Powders of C₆Br₆ and α -Fe₂O₃ nanoparticles (1:2 in weight ratio) were mixed together by first dissolving C₆Br₆ in chloroform, then adding Fe₂O₃ particles and stirring, and finally evaporating the solvent. After powders were annealed at 250 °C in pure hydrogen flow, the weight ratio of C₆Br₆ and iron oxide nanoparticles changed to about 1:15 owing to the sublimation of C₆Br₆. Further annealing at 250 °C does not change the weight ratio significantly. The annealed powders were then pressed into pellets under a pressure of 5×10^8 N/m². The samples were annealed again in pure hydrogen flow. For the samples used in the transport measurement, contacts were made on the pellets and a PS layer was coated on the surface to protect the pellet before annealing. X-ray diffraction (XRD) patterns were collected with a Philips X'Pert diffractometer using Cu $K\alpha$ radiation. Transmission electron microscopy (TEM) was done with a JEOL 2010 TEM. Samples destined for TEM analysis were prepared by ultrasonic dispersion of the annealed pellets in water, and a drop of suspension solution was placed on a holey carbon film grid. The resistance (R) and MR of the pellet samples were measured with a standard four-point method using a Quantum Design physical property measurement system. A magnetic field of up to 5 T was applied perpendicular to the current.

^{a)}Electronic mail: wwang3@uwyo.edu.

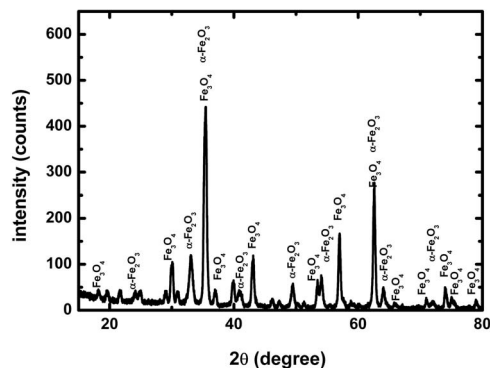


FIG. 1. XRD patterns of magnetite/ C_6Br_6 nanocomposite, annealed at 250 °C in pure hydrogen flow.

Figure 1 is the XRD pattern of the sample annealed at 250 °C in hydrogen. The pattern shows that there exist Fe_3O_4 (or $\gamma-Fe_2O_3$) and a small amount of $\alpha-Fe_2O_3$. The rest of the peaks do not fit the published pattern of monoclinic C_6Br_6 . However, it may be possible that the structure of C_6Br_6 thin layer coated on the iron oxide is different from the bulk molecular crystals. There have been reports that the structure of C_6Br_6 films grown on graphite is hexagonal.²³ Figure 2 is the TEM image of the sample annealed at 250 °C. It shows that Fe_3O_4 (or $\gamma-Fe_2O_3$) particles are nearly spherical and their sizes are between 10 and 30 nm.

The samples before annealing were insulators. After annealing in pure hydrogen, the samples became conducting. Knowing that $\gamma-Fe_2O_3$ is an insulator, the $\alpha-Fe_2O_3$ should transform to magnetite after reduction in hydrogen. The magnetization M of the samples also shows the unique character of the Verwey transition (a sudden drop in M at the transition), which supports that the sample has transformed from $\alpha-Fe_2O_3$ to Fe_3O_4 .

The temperature dependence of the resistance for an annealed sample is shown in Fig. 3(a). In Fe_3O_4 , the Verwey transition is characterized by an increase in resistivity by about two orders of magnitude at the transition temperature $T_V \sim 120$ K. In our samples the change in the resistance at Verwey transition is not as sharp as those observed in single crystal samples. In Fig. 3(b), R is plotted on a logarithmic scale as a function of $T^{-1/2}$. The good linear behavior suggests intergranular tunneling is the mechanism of transport.⁵

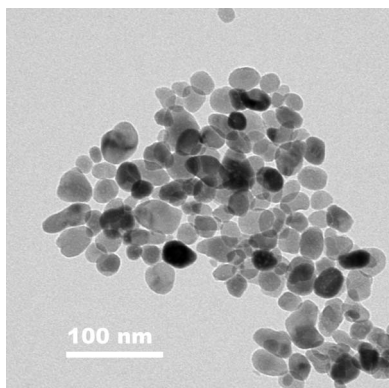


FIG. 2. TEM image of magnetite/ C_6Br_6 nanocomposite annealed at 250 °C.

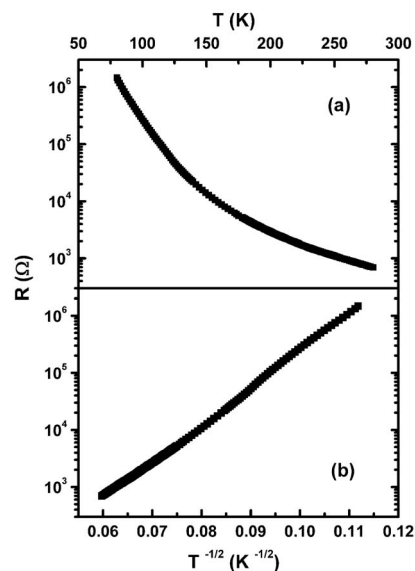


FIG. 3. Resistance as a function of temperature for magnetite/ C_6Br_6 nanocomposite samples: (a) logarithmic R - T plot and (b) logarithmic R - $T^{-1/2}$ plot.

Figure 4 shows the $MR = (R_H - R_0)/R_0$ of the sample annealed at 250 °C. Giant negative MR was observed at room temperature (280 K) and the MR ratio is 13.4% in an applied field of 5 T. The MR ratio is 21.5% at 130 K; however it slightly decreases to 19.4% at 85 K. Although the existence of $\alpha-Fe_2O_3$ should decrease MR effect, these MR values are higher than reported data in pressed Fe_3O_4 powders and polycrystalline films,^{9,24-26} which have MR ratios typically near 4%–5% at room temperature. It is well known that the surface state of Fe_3O_4 is different from the bulk. X-ray photoelectron spectroscopy study indicates that the top two layers of surface are rich in Fe (III) compared to the bulk in molecular beam epitaxy-grown Fe_3O_4 film.²⁷ In our sample, a reasonable explanation of enhanced MR is that a thin layer of C_6Br_6 is perhaps coated on the surface of Fe_3O_4 , which may help to prevent the oxidation of the surface of Fe_3O_4 . The latter may have altered half-metallic state at its surface. We have previously mentioned that after primary sublimation of C_6Br_6 , further annealing will not change the weight ratio between C_6Br_6 and Fe_3O_4 . This implies that there may be some sort of binding between C_6Br_6 and the surface of iron oxide. Further investigation of the morphology of C_6Br_6 on iron oxide will be performed.

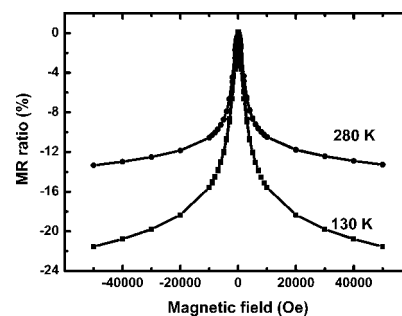


FIG. 4. MR as a function of magnetic field at 130 and 280 K for the sample annealed at 250 °C.

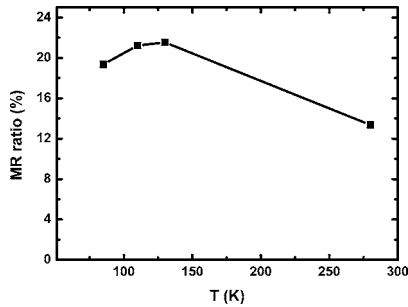


FIG. 5. Temperature dependence of the MR ratio in an applied field of 5 T for the sample annealed at 250 °C.

Figure 5 shows the temperature dependence of MR ratio in an applied field of 5 T. In our samples, MR ratios before and after Verwey point do not show significant change, implying that Verwey transition does not change the spin polarization of Fe_3O_4 significantly.

Our investigation suggests that C_6Br_6 can improve the MR performance of Fe_3O_4 . Since this organic material has been successfully applied to growth of molecular films, it is possible that it can be used on Fe_3O_4 thin film systems and to improve their spin polarized characteristics.

ACKNOWLEDGMENTS

This work was supported by NSF and the School of Energy Resources of the University of Wyoming (Contract No. DMR-0852862)

¹A. M. Bratkovsky, *Phys. Rev. B* **56**, 2344 (1997).

²A. M. Bratkovsky, *Appl. Phys. Lett.* **72**, 2334 (1998).

³S. Mitani, S. Takahashi, K. Takanashi, K. Yakushiji, S. Maekawa, and H. Fujimori, *Phys. Rev. Lett.* **81**, 2799 (1998).

⁴X. W. Li, A. Gupta, G. Xiao, W. Qian, and V. P. Dravid, *Appl. Phys. Lett.* **73**, 3282 (1998).

⁵J. Inoue and S. Maekawa, *Phys. Rev. B* **53**, R11927 (1996).

⁶V. V. Gridin, G. R. Hearne, and J. M. Honig, *Phys. Rev. B* **53**, 15518 (1996).

⁷W. Eerenstein, T. T. M. Palstra, S. S. Saxena, and T. Hibma, *Phys. Rev. Lett.* **88**, 247204 (2002).

⁸W. Eerenstein, T. T. M. Palstra, T. Hibma, and S. Celotto, *Phys. Rev. B* **66**, 201101(R) (2002).

⁹J. M. D. Coey, A. E. Berkowitz, L. Balcells, F. F. Putris, and F. T. Parker, *Appl. Phys. Lett.* **72**, 734 (1998).

¹⁰D. L. Peng, T. Asai, N. Nozawa, T. Hihara, and K. Sumiyama, *Appl. Phys. Lett.* **81**, 4598 (2002).

¹¹J. J. Versluijs, M. A. Bari, and J. M. D. Coey, *Phys. Rev. Lett.* **87**, 026601 (2001).

¹²P. Poddar, T. Fried, and G. Markovich, *Phys. Rev. B* **65**, 172405 (2002).

¹³J. M. De Teresa, A. Barh el my, A. Fert, J. P. Contour, F. Montaigne, and P. Seneor, *Science* **286**, 507 (1999).

¹⁴J. H. Park, E. Vescovo, H.-J. Kim, C. Kwon, R. Ramesh, and T. Venkatesan, *Phys. Rev. Lett.* **81**, 1953 (1998).

¹⁵H. Dulli, E. W. Plummer, P. A. Dowben, J. Choi, and S. H. Liou, *Appl. Phys. Lett.* **77**, 570 (2000).

¹⁶S. I. Rybchenko, Y. Fujishiro, H. Takagi, and M. Awano, *Phys. Rev. B* **72**, 054424 (2005).

¹⁷H. Zeng, C. T. Black, R. L. Sandstrom, P. M. Rice, C. B. Murray, and S. Sun, *Phys. Rev. B* **73**, 020402(R) (2006).

¹⁸W. Wang, M. Yu, M. Batzill, J. He, U. Diebold, and J. Tang, *Phys. Rev. B* **73**, 134412 (2006).

¹⁹S. I. Rybchenko, Y. Fujishiro, H. Takagi, and M. Awano, *Appl. Phys. Lett.* **89**, 132509 (2006).

²⁰Z. L. Lu, M. X. Xu, W. Q. Zou, S. Wang, X. C. Liu, Y. B. Lin, J. P. Xu, Z. H. Lu, J. F. Wang, L. Y. Lv, F. M. Zhang, and Y. W. Du, *Appl. Phys. Lett.* **91**, 102508 (2007).

²¹K. Mohan Kant, K. Sethupathi, and M. S. Ramachandra Rao, *J. Appl. Phys.* **103**, 07F318 (2008).

²²W. Wang, L. Malkinski, and J. Tang, *J. Appl. Phys.* **101**, 09J504 (2007).

²³D. E. Hooks, T. Fritz, and M. D. Ward, *Adv. Mater. (Weinheim, Ger.)* **13**, 227 (2001).

²⁴J. Tang, K.-Y. Wang, and W. Zhou, *J. Appl. Phys.* **89**, 7690 (2001).

²⁵H. Liu, E. Y. Jiang, H. L. Bai, R. K. Zheng, H. L. Wei, and X. X. Zhang, *Appl. Phys. Lett.* **83**, 3531 (2003).

²⁶D. Serrate, J. M. De Teresa, P. A. Algarabel, R. Fern andez-Pacheco, J. Galibert, and M. R. Ibarra, *J. Appl. Phys.* **97**, 084317 (2005).

²⁷S. A. Chambers, S. Thevuthasan, and S. S. Joyce, *Surf. Sci.* **450**, L273 (2000).